Electronic structures and optical properties of III_A-doped wurtzite $Mg_{0.25}Zn_{0.75}O$*

Zheng Shu-Wen(郑树文)†, He Miao(何 苗), Li Shu-Ti(李述体), and Zhang Yong(章 勇)

Laboratory of Nanophotonic Functional Materials and Devices, Institute of Opto-electronic Materials and Technology, South China Normal University, Guangzhou 510631, *China*

(Received 10 March 2014; revised manuscript received 8 May 2014; published online 10 June 2014)

The energy band structures, density of states, and optical properties of III_A-doped wurtzite $Mg_{0.25}Zn_{0.75}O$ (III_A = Al, Ga, In) are investigated by a first-principles method based on the density functional theory. The calculated results show that the optical bandgaps of $Mg_{0.25}Zn_{0.75}O$:III_A are larger than those of $Mg_{0.25}Zn_{0.75}O$ because of the Burstein–Moss effect and the bandgap renormalization effect. The electron effective mass values of $Mg_{0.25}Zn_{0.75}O$:III_A are heavier than those of $Mg_{0.25}Zn_{0.75}O$, which is in agreement with the previous experimental result. The formation energies of MgZnO:Al and MgZnO:Ga are smaller than that of MgZnO:In, while their optical bandgaps are larger, so MgZnO:Al and MgZnO:Ga are suitable to be fabricated and used as transparent conductive oxide films in the ultra-violet (UV) and deep UV optoelectronic devices.

Keywords: first-principles, $Mg_{0.25}Zn_{0.75}O$, electronic structure, optical bandgap

PACS: 71.15.Mb, 73.20.At, 74.20.Pq, 72.15.–v **DOI:** 10.1088/1674-1056/23/8/087101

1. Introduction

Transparent conductive oxide (TCO) material plays an important role in the optoelectronics industry, and it is used as window film or electrode film in light-emitting diode, laser diode, solar cell, and detector. At present, ITO (In_2O_3:Sn) is a widely used material for TCO applications, though indium is rare and expensive. ZnO is one of the most promising candidates to replace ITO because it is a nontoxic, cheap, and relatively abundant material. Intrinsic ZnO has a wide bandgap of 3.37 eV,[1] transparency in the visible range, and high conductivity of n-type ZnO thin films are readily obtained by doping with III_A donor elements to displace zinc sites, such as Al, Ga, and In.[2]

However, various device applications require higher optical transmittance in the wider light range, especially in the UV range, so we need to develop wider bandgap material for TCO applications. Moreover, a TCO with wider band gap can improve the efficiency of UV and blue light emitting device when used as a transparent electrode,[3] it can also be designed as conducting oxide heterostructures to increase electron mobility.[4] The bandgap of ZnO can be enlarged by increasing the Mg content in $Mg_xZn_{1-x}O$. Ohtomo *et al.*[5] reported that the bandgap of $Mg_xZn_{1-x}O$ can be tuned up to 3.99 eV at room temperature (RT) when the Mg content x is 0.33. But $Mg_xZn_{1-x}O$ has high resistivity and is not suited to be used as a TCO material for optoelectronics devices, so several research groups have focused on n-type $Mg_xZn_{1-x}O$ film recently. Matsubara *et al.*[3] reported that the average transmittance of Al-doped $Mg_xZn_{1-x}O$ film deposited by pulsed laser deposition was over 90% in the 400-nm∼800-nm wavelength region and its maximum bandgap is 3.97 eV. Yang *et al.*[6] reported that Al-doped $Mg_xZn_{1-x}O$ film possessed the lowest resistivity of 3.2×10^{-4} Ω·cm (corresponding carrier concentration is as high as 1×10^{21} cm^{-3}) and its bandgap can be increased from 3.78 eV to 4.66 eV with the increase of Mg content from 0.1 to 0.3. Tian *et al.*[7] deposited Ga-doped $Mg_xZn_{1-x}O$ film via pulsed direct current reactive magnetron sputtering on glass substrates and found that its bandgap can be adjusted from 3.49 eV to 3.7 eV by changing the Mg content, and the lowest resistivity of $Mg_xZn_{1-x}O$:Ga film is 7.4×10^{-3} Ω·cm. Liu *et al.*[8] reported that a high optical transmittance of Ga-doped $Mg_xZn_{1-x}O$ film deposited by radio-frequency magnetron sputtering was over 96.6% in the wavelength range between 350 nm and 1100 nm, and the resistivity is 5.69×10^{-4} Ω·cm along with a carrier concentration of 3.85×10^{20} cm^{-3}. Compared with the studies of Al or Ga-doped $Mg_xZn_{1-x}O$, the research on In-doped $Mg_xZn_{1-x}O$ is limited. Cohen *et al.*[9] reported that Al and In co-doped $Mg_xZn_{1-x}O$ film has higher conductivity and larger mobility than Al-doped $Mg_xZn_{1-x}O$, but this mechanism is unclear. In order to better understand the properties of Al, Ga or In-doped $Mg_xZn_{1-x}O$, the electronic structures and optical properties of III_A-doped $Mg_{0.25}Zn_{0.75}O$ are caculated, compared, and analysed systematically in this paper.

*Project supported by the National Natural Science Foundation of China (Grant No. 61078046), the Special Funds for Provincial Strategic and Emerging Industries Projects of Guangdong Province, China (Grant No. 2012A080304016), and the Youth Foundation of South China Normal University, China (Grant No. 2012KJ018).

†Corresponding author. E-mail: LED@scnu.edu.cn

© 2014 Chinese Physical Society and IOP Publishing Ltd

2. Computational methods

In this paper, the energy band structures, density of states and optical properties are performed by using the first-principles plane-wave pseudo-potential method based on the density functional theory (DFT) as implemented in the CASTEP package.[10] The exchange–correlation effects are employed through the generalized gradient approximation (GGA) within the Perdew–Burke–Ernzerhof (PBE) function.[11] The atomic cores are described by the ultra-soft pseudopotential, and the valence atomic configurations are Zn $3d^{10}4s^2$, Mg $3s^2$, O $2s^2 2p^4$, Al $3s^2 3p^1$, Ga $3d^{10}4s^2 4p^1$, and In $4d^{10}5s^2 5p^1$, respectively. The convergence test of the total energy with respect to the plane-wave cut-off energy and *k*-point sampling is carefully examined. The final set of cut-off energy is 400 eV for the calculation of energy band structure and density of state, while 550 eV is for the calculation of optical absorption. The 6×6×4 *k*-point Monkhorst–Pack[12] mesh is found to be sufficient for the Brillouin zone integration in reciprocal space.

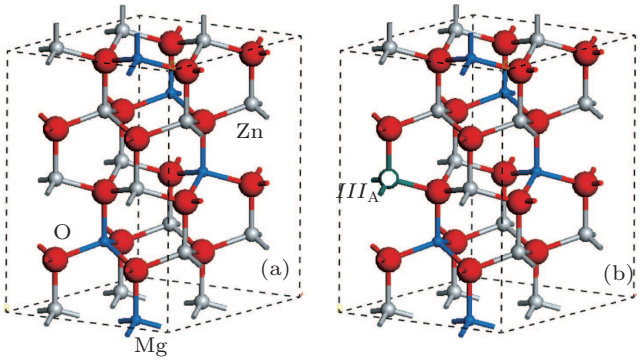


Fig. 1. (color online) Structural models for wurtzite $Mg_{0.25}Zn_{0.75}O$ (a) and III_A-doped $Mg_{0.25}Zn_{0.75}O$ (b), the III_A refers to Al, Ga or In atom.

In order to simulate the wurtzite $Mg_{0.25}Zn_{0.75}O$ and III_A-doped $Mg_{0.25}Zn_{0.75}O$, our computational models are shown in Fig. 1. According to the special quasirandom structures (SQS) approach,[13] the 32-atom supercell of wurtzite (2×2×2) ZnO is used to obtain $Mg_{0.25}Zn_{0.75}O$ by replacing four Zn sites with four Mg atoms, which can be seen in Fig. 1(a), and III_A-doped MgZnO by replacing five Zn sites with four Mg atoms and one III_A atom; the corresponding III_A doping concentration is 3.125 at.%, as shown in Fig. 1(b), where the III_A element specifically refers to Al, Ga or In, and III_A-doped MgZnO can be written simply as MgZnO:Al, MgZnO:Ga or MgZnO:In. To ensure the structural configurations of the above models converge to their stable conformation, all atomic positions and lattice constants are relaxed and optimized by the BFGS[14] until the total energy converges to less than 1.0×10^{-5} eV/atom. The final atomic positions of the structural models are strictly determined by a high-symmetry configuration and the lowest total energy.

3. Results and discussion

3.1. Structural properties

For comparison, the wurtzite $Mg_{0.25}Zn_{0.75}O$ alloy is first calculated. The structural parameters and supercell total energies of $Mg_{0.25}Zn_{0.75}O$ are listed in Table 1. It can be seen that the calculated lattice constants of $Mg_{0.25}Zn_{0.75}O$ are in good agreement with the experimental and other calculated data reported in Refs. [5] and [15], which indicates that the calculated method and models are rational. The structural parameters and supercell total energies of MgZnO:Al, MgZnO:Ga, and MgZnO:In are also given in Table 1. It is evident that the supercell volume of MgZnO:Al is slightly smaller than that of $Mg_{0.25}Zn_{0.75}O$, but the supercell volumes of MgZnO:Ga and MgZnO:In are bigger than that of $Mg_{0.25}Zn_{0.75}O$, which can be explained according to the competitive effects: the Coulomb repulsion and the ionic radius difference between III_A and Zn. When the Zn atom is replaced by the III_A atom, excess free electrons will occur and make the Coulomb repulsion enhanced, and the strong effect of Coulomb repulsion will increase the supercell volume. For MgZnO:Al, the Al ionic radius (0.39 Å) is much smaller than the Zn ionic radius (0.60 Å) and makes the supercell volume smaller when replacing the Zn^{2+} site by Al^{3+}, so the two competitivities cause the supercell volume of MgZnO:Al to be smaller than that of $Mg_{0.25}Zn_{0.75}O$. A similar analysis can be used to explain the supercell volume changes of MgZnO:Ga and MgZnO:In.

Table 1. Calculated structural parameters, supercell total energies, and formation energies of wurtzite $Mg_{0.25}Zn_{0.75}O$, MgZnO:Al, MgZnO:Ga, and MgZnO:In.

Name		lattice constant		Supercell	Supercell	Formation energy E_f/(eV/pair)	
		a/Å	*c*/Å	volume/Å^3	total energy/eV	O-rich	Zn-rich
$Mg_{0.25}Zn_{0.75}O$	This work	3.292	5.284	396.702	–31422.794		
	Exp.[5]	3.254	5.183				
	Calc.[15]	3.283	5.267				
MgZnO:Al		3.297	5.280	396.581	–29771.519	0.171	–0.132
MgZnO:Ga		3.299	5.304	400.418	–31765.277	0.157	0.03
MgZnO:In		3.320	5.340	408.306	–31272.087	0.174	0.102

As seen from Table 1, the supercell total energy of MgZnO:Ga is smaller than that of $Mg_{0.25}Zn_{0.75}O$, but it is a contrary scenario for MgZnO:Al and MgZnO:In. This reveals that doping Ga into $Mg_{0.25}Zn_{0.75}O$ helps enhance the structural stability, while doping Al or In into $Mg_{0.25}Zn_{0.75}O$ causes the structural stability to decline. The formation energy is an important material parameter and is often used to evaluate the difficulty in forming a doped material system. If the formation energy is positive, it means that the doped material system is difficult to obtain. If the formation energy is negative, it means that the doped system can be easily fabricated. The formation energies of MgZnO:III_A are defined by the following formula[16]

$$E_f = E_{tot}(MgZnO : III_A) - E_{tot}(Mg_{0.25}Zn_{0.75}O) + \mu_{Zn} - \mu_{III_A}, \quad (1)$$

where $E_{tot}(MgZnO : III_A)$ and $E_{tot}(Mg_{0.25}Zn_{0.75}O)$ are the calculated total energies of MgZnO:III_A and $Mg_{0.25}Zn_{0.75}O$, respectively, while μ_{Zn} and μ_{III_A} are the chemical potentials of Zn and III_A, respectively. The formation energy is not fixed but depends on the growth condition,[17] which can be either an O-rich condition or a Zn-rich condition. The Zn and III_A chemical potentials are taken from the previous calculated method.[18] The calculated formation enthalpy for ZnO is −3.489 eV, which is in agreement with its experimental value of −3.58 eV.[19] By Eq. (1), the formation energies of MgZnO:III_A in O-rich and Zn-rich conditions are calculated and listed in Table 1. It is clear that the formation energies of MgZnO:III_A in the Zn-rich condition is much lower than in the O-rich condition, which indicates that good MgZnO:III_A material is more likely to be prepared in the Zn-rich condition. Furthermore, we notice that the formation energy of MgZnO:Al in the Zn-rich condition is negative, so MgZnO:Al is easy to grow in the Zn-rich condition. The formation energies of MgZnO:Ga and MgZnO:In are positive in O-rich and Zn-rich conditions, but the formation energy of MgZnO:Ga is small in the Zn-rich condition, so MgZnO:Ga can be fabricated by improving the experimental condition, such as the growth temperature.

3.2. Energy band structure and density of state

The energy band structures of wurtzite $Mg_{0.25}Zn_{0.75}O$ and MgZnO:III_A are calculated and given in Fig. 2. As can be seen in Fig. 2(a), the Fermi level of $Mg_{0.25}Zn_{0.75}O$ is at the top of the valence band and is defined as being 0 eV. The bottom of the conduction band and the top of the valence band of $Mg_{0.25}Zn_{0.75}O$ are located at the same symmetry point (G), which indicates that wurtzite $Mg_{0.25}Zn_{0.75}O$ is a direct-bandgap semiconductor, and its energy bandgap is about 1.339 eV, which is smaller than its experimental value (3.855 eV[5]). In fact, underestimation of the energy bandgap is a well-known drawback by the standard DFT calculation, but the bandgap can be corrected by the scissors

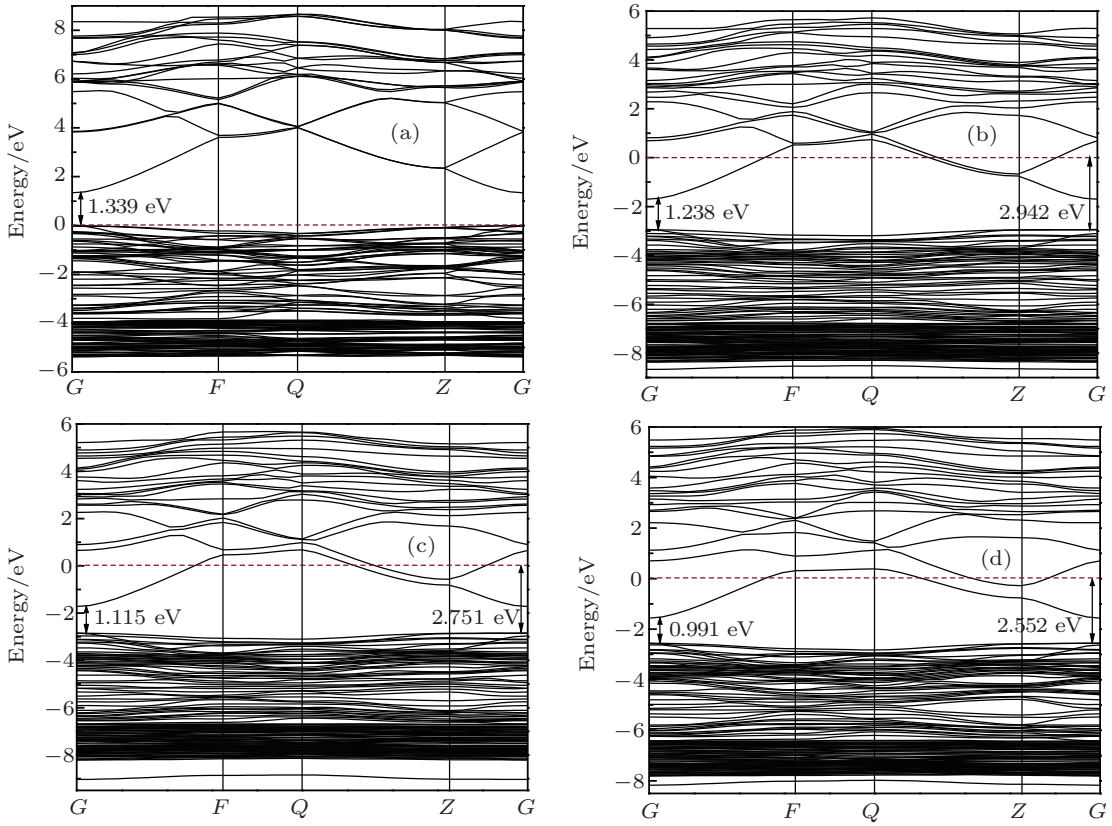


Fig. 2. Calculated band structures of wurtzite $Mg_{0.25}Zn_{0.75}O$ (a), MgZnO:Al (b), MgZnO:Ga (c), and MgZnO:In (d). The k symmetry points are G (0,0,0), F (0,0.5,0), Q (0,0.5,0.5), and Z (0, 0,0.5). Fermi level indicated by a horizontal dashed line is set to be zero.

approximation.[20] Our calculated energy bandgap of wurtzite $Mg_{0.25}Zn_{0.75}O$ is consistent with previous results.[15,21] From Figs. 2(b) to 2(d), we can see that the energy bandgaps of MgZnO:Al, MgZnO:Ga, and MgZnO:In are 1.238 eV, 1.115 eV, and 0.991 eV respectively, which are narrower than the bandgap of $Mg_{0.25}Zn_{0.75}O$. It is interesting that the energy bandgap decreases gradually with the increase in III_A-group atomic number. Moreover, we notice that the Fermi level enters into the conduction band when the Zn atom is replaced by the III_A atom, which is attributed to the bottom of the conduction band filled by excess free electrons.

The total densities of states (DOSs) of wurtzite $Mg_{0.25}Zn_{0.75}O$ and MgZnO:III_A are plotted in Fig. 3. It is observed that the Fermi levels shift obviously and enter into the conduction bands of MgZnO:III_A when doping III_A into $Mg_{0.25}Zn_{0.75}O$, which are consistent with the energy band structures. As mentioned above, the Fermi level shift is derived from the states at the bottom of the conduction band occupied by excess free electrons, so the electron number of the conduction band can be obtained according to the integrated area between the Fermi level and the bottom of the conduction band of the total DOS.[22] The electron number of MgZnO:III_A can be expressed as n'_{III_A}, and the values of supercell volume (V_{III_A}) of MgZnO:III_A are given in Table 1, so the electron concentration (n_e) of MgZnO:III_A can be defined as $n_e = n'_{III_A}/V_{III_A}$. According to the total DOS in Fig. 3, the values of electron concentration (n_e) of MgZnO:Al, MgZnO:Ga, and MgZnO:In are calculated to be 2.884×10^{21}, 2.735×10^{21}, and 2.563×10^{21} cm^{-3}, respectively.

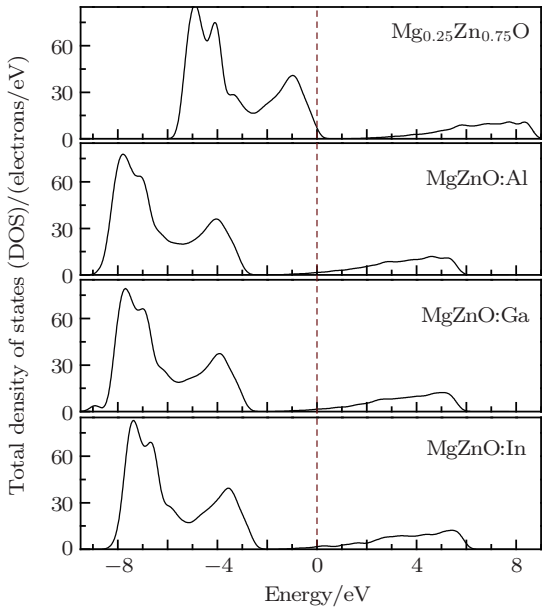


Fig. 3. Total DOSs of wurtzite $Mg_{0.25}Zn_{0.75}O$, MgZnO:Al, MgZnO:Ga, and MgZnO:In. The Fermi level indicated by a vertical dashed line is set to be zero.

3.3. Optical properties

It is well known that the optical bandgap of a material can be obtained based on its transmittance spectra or absorption spectra. In fact, the optical bandgap of a material can also be gained according to its energy band structure. As can be seen from Fig. 2(a), the energy bandgap of wurtzite $Mg_{0.25}Zn_{0.75}O$ is 1.339 eV, which is equal to its optical bandgap because the electron vertical transition occurs mainly between the top of the valence band and the bottom of the conduction band. But for n-type MgZnO, because excess free electrons fill the bottom of its conduction band and the Fermi level enters into the conduction band, so the electron transition occurs chiefly between the top of the valence band and the Fermi level,[23] which makes the optical bandgaps of MgZnO:III_A unequal to their energy bandgaps. As seen in Fig. 2, the optical bandgaps of MgZnO:Al, MgZnO:Ga, and MgZnO:In are 2.942 eV, 2.751 eV, and 2.552 eV, respectively. It is obvious that the optical bandgaps of MgZnO:III_A are larger than their energy bandgaps and those of $Mg_{0.25}Zn_{0.75}O$, so doping III_A into $Mg_{0.25}Zn_{0.75}O$ can increase its optical bandgap, which is in agreement with the reported experimental results.[6–9]

For the doped semiconductor with heavily doping concentration (i.e., $> 10^{19}$ cm^{-3}), there are primarily two competing mechanisms affecting its optical bandgap: the Burstein–Moss effect[24,25] and the bandgap renormalization effect.[26,27] The optical bandgap (E_g^o) can be written as follows:[23]

$$E_g^o = E_{go} + \Delta E_{BM} - \Delta E_{BGN}, \tag{2}$$

where E_{go} is the energy bandgap of wurtzite $Mg_{0.25}Zn_{0.75}O$, ΔE_{BM} is the bandgap widening due to the Burstein–Moss Fermi-band filling effect, and ΔE_{BGN} is the bandgap narrowing due to the many-body bandgap renormalization effect and the semiconductor–metal transition effect. Based on Eq. (2) and the energy band structures of $Mg_{0.25}Zn_{0.75}O$ and MgZnO:III_A (see Fig. 1), the calculated data of ΔE_{BM} and ΔE_{BGN} of MgZnO:III_A are obtained and listed in Table 2. The data indicate that the Burstein–Moss effect is much stronger than the bandgap renormalization effect. It is also found from Table 2 that ΔE_{BM} decreases gradually with the increase in III_A-group atomic number but it is the opposite scenario for ΔE_{BGN}, so the optical bandgap of MgZnO:Al is larger than those of MgZnO:Ga and MgZnO:In under the same doping concentration. Although the optical bandgaps of $Mg_{0.25}Zn_{0.75}O$ and MgZnO:III_A are underestimated by DFT with generalized gradient approximation (GGA) and local density approximation (LDA), it can be corrected by the scissors approximation. The scissor value is set to be 2.516 eV according to the difference between the experimental value (3.855 eV[5]) and the calculated result (1.339 eV) of $Mg_{0.25}Zn_{0.75}O$. The corrected optical bandgaps of MgZnO:Al, MgZnO:Ga, and MgZnO:In are 5.458 eV, 5.267eV, and 5.068 eV, which are much larger than that of $Mg_{0.25}Zn_{0.75}O$, so MgZnO:III_A material can be used in the UV and deep UV optoelectronic devices.

Table 2. Calculated optical bandgaps of MgZnO:III_A under the Burstein–Moss effect ΔE_{BM} and many-body renormalization effect ΔE_{BGN}, and the optical bandgaps are corrected by the scissors approximation (the scissor value is 2.516 eV).

Name	$Mg_{0.25}Zn_{0.75}O$	MgZnO:Al	MgZnO:Ga	MgZnO:In
$n_e/10^{21}$ cm^{-3}	0	2.884	2.735	2.563
ΔE_{BM}/eV	0	1.704	1.636	1.562
ΔE_{BGN}/eV	0	0.101	0.224	0.348
E_g^{opt}/eV	1.339	2.942	2.751	2.552
Corrected E_g^{opt}/eV	3.855	5.458	5.267	5.068

In order to better understand the optical bandgaps of $Mg_{0.25}Zn_{0.75}O$ and MgZnO:III_A, the absorption spectra of $Mg_{0.25}Zn_{0.75}O$ and MgZnO:III_A are calculated through the Kramers–Kronig relations[28] and corrected by the scissors approximation, as shown in Fig. 4. The optical bandgap (E_g^o) can also be estimated by the Tuac relationship[29] between the absorption coefficient (α) and the photon energy ($h\nu$) given as follows:

$$\alpha h\nu = A(h\nu - E_g^o)^{1/2}. \tag{3}$$

Here ν is the frequency of radiation and A is a constant. Equation (3) gives the optical bandgaps of $Mg_{0.25}Zn_{0.75}O$ and MgZnO:III_A while the straight portion of $(\alpha h\nu)^2$ is plotted against $h\nu$, and extrapolated to $\alpha = 0$. As shown in Fig. 5, the optical bandgap of $Mg_{0.25}Zn_{0.75}O$ is 3.816 eV, and the optical bandgaps of MgZnO:Al, MgZnO:Ga, and MgZnO:In are 5.448 eV, 5.346 eV, and 5.048 eV, respectively. It is clear that the optical bandgaps deduced from the absorption spectra are consistent with the optical bandgaps obtained from the energy band structures. The optical bandgaps of MgZnO:Al, MgZnO:Ga are much larger than the optical bandgap of MgZnO:In, so MgZnO:Al and MgZnO:Ga have the advantage over MgZnO:In in serving as TCO films for short-wavelength optoelectronic devices.

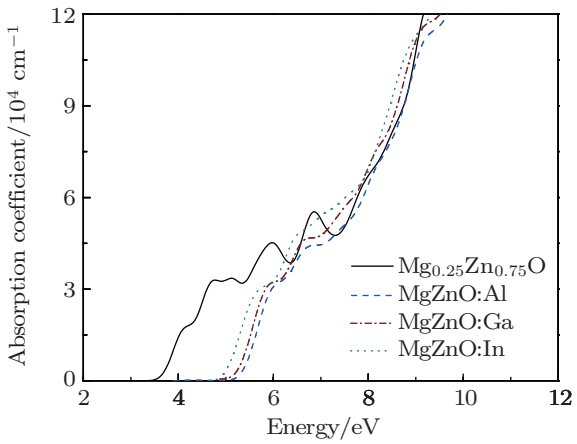


Fig. 4. Calculated absorption spectra of wurtzite $Mg_{0.25}Zn_{0.75}O$, MgZnO:Al, MgZnO:Ga, and MgZnO:In.

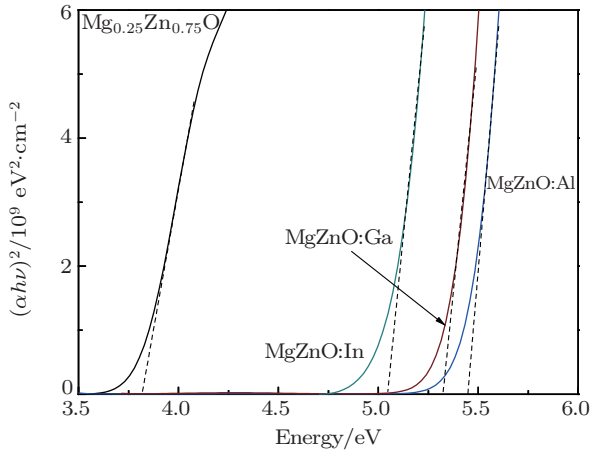


Fig. 5. Plots of $(\alpha h\nu)^2$ versus photon energy of wurtzite $Mg_{0.25}Zn_{0.75}O$, MgZnO:Al, MgZnO:Ga, and MgZnO:In.

3.4. Electron effective mass

According to the above analysis of the energy band structure and DOS, for $Mg_{0.25}Zn_{0.75}O$ alloy, the electronic interband transition occurs chiefly between the top of the valence band and the bottom of the conduction band, so the electron effective mass (m_e^*) of $Mg_{0.25}Zn_{0.75}O$ can be calculated from the following equation:

$$m_e^* = \frac{h^2}{4\pi^2}\left(\frac{d^2E}{dk^2}\right)^{-1}, \tag{4}$$

where h is the Planck constant, E and k are the energy and wave vector, respectively. In terms of Eq. (4) and the energy band structure of $Mg_{0.25}Zn_{0.75}O$, as seen in Fig. 1(a), the electron effective mass corresponding to the G point of the band structure is calculated to be $0.423m_0$ (m_0 is the electron mass). But for the n-type doped material system, the bottom of the conduction band is filled by the excess free electrons, the electronic transition occurs mainly between the Fermi level and the top of the valence band,[23] and the conduction band is a nonparabolic band,[30] so the electron effective mass of an n-type material system cannot be obtained by Eq. (4). According to the Burstein–Moss effect model,[31,32] the relationship between the electron effective mass and electron concentration is expressed as

$$\Delta E_{BM} = \frac{h^2}{8m_e^*}\left(\frac{3n_e}{\pi}\right)^{2/3}. \tag{5}$$

Based on the above calculated results of ΔE_{BM} and n_{e} (see Table 2), the electron effective mass values of MgZnO:Al, MgZnO:Ga, and MgZnO:In are calculated from Eq. (5), and their values are $0.434m_0$, $0.436m_0$, and $0.437m_0$, respectively. The electron effective mass values of MgZnO:III_{A} are heavier than those of $Mg_{0.25}Zn_{0.75}O$, which is in agreement with the recent experimental result.[33]

4. Conclusion

The energy band structures, densities of states, optical properties, and electron effective mass values of wurtzite $Mg_{0.25}Zn_{0.75}O$ and III_{A}-doped $Mg_{0.25}Zn_{0.75}O$ (III_{A} = Al, Ga, In) are calculated, compared, and analyzed systematically by the first-principles method. The results show that the optical bandgaps of $Mg_{0.25}Zn_{0.75}O$:III_{A}, obtained from the energy band structures, are consistent with those from the absorption spectra, and are larger than those of $Mg_{0.25}Zn_{0.75}O$, which results from the Burstein–Moss effect and the bandgap renormalization effect. The electron effective mass values of $Mg_{0.25}Zn_{0.75}O$:III_{A} are heavier than those of $Mg_{0.25}Zn_{0.75}O$, which is in agreement with the experimental result. Because the formation energies of MgZnO:Al and MgZnO:Ga are smaller than the formation energy of MgZnO:In, but their optical bandgaps are larger, MgZnO:Al and MgZnO:Ga are suited to grow and serve as TCO films for UV and deep UV optoelectronic devices.

References

[1] Yang Z H, Zheng J H, Zhai H J, Yang L L, Liu L and Gao M 2009 *Cryst. Res. Technol.* **44** 619
[2] Wang F, Chen X L, Geng X H, Zhang D K, Wei C C, Huang Q, Zhang X D and Zhao Y 2012 *Appl. Surf. Sci.* **258** 9005
[3] Matsubara K, Tampo H, Shibata H, Yamada A, Fons P, Iwata K and Niki S 2004 *Appl. Phys. Lett.* **85** 1374
[4] Robbins J J and Wolden C A 2003 *Appl. Phys. Lett.* **83** 3933
[5] Ohtomo A, Kawasaki M, Koida T, Masubuchi K, Koinuma H, Sakurai Y, Yoshida Y, Yasuda T and Segawa Y 1998 *Appl. Phys. Lett.* **72** 2466
[6] Yang C, Li X M, Gao X D, Cao X, Yang R and Li Y Z 2011 *Solid State Commun.* **151** 264
[7] Tian C S, Chen X L, Liu J M, Zhang D K, Wei C C, Zhao Y and Zhang X D 2014 *Acta Phys. Sin.* **63** 036801 (in Chinese)
[8] Liu W S, Chen W K and Hsueh K P 2013 *J. Alloys Compd.* **552** 255
[9] Cohen D J, Ruthe K C and Barnett S A 2004 *J. Appl. Phys.* **96** 459
[10] Segall M D, Lindan P, Probet M J, Pickard C J, Hasnip P J, Clark S J, and Payne M C 2002 *J. Phys.: Condens. Matter* **14** 2717
[11] Perdew J, Burke K and Ernzerhof M 1996 *Phys. Rev. Lett.* **77** 3865
[12] Monkhorst H J and Pack J D 1976 *Phys. Rev. B* **13** 5188
[13] Zunger A, Wei S H, Ferreira L G and Bemard J E 1990 *Phys. Rev. Lett.* **65** 353
[14] Fischer T H and Almlof J 1992 *J. Phys. Chem.* **96** 9768
[15] Wang Z J, Li S C, Wang L T and Liu Z 2009 *Chin. Phys. B* **18** 2992
[16] Yang K S, Dai Y and Huang B B 2008 *Chem. Phys. Lett.* **456** 71
[17] Van de Walle C G and Neugebauer J 2004 *J. Appl. Phys.* **95** 3851
[18] Saniz R, Xu Y, Matsubara M, Amini M N, Dixit H, Lamoen and Partoens B 2013 *J. Phys. Chem Solids* **74** 45
[19] Dean J A 1992 *Lange's Handbook of Chemistry*, 14th edn. (New York: McGraw-Hill, Inc.)
[20] Yoo Y Z, Jin Z W, Chikyow T, Fukumura T, Kawasaki M and Koinuma H 2002 *Appl. Phys. Lett.* **81** 3798
[21] Huang D, Shao Y Z, Chen D H, Guo J and Li G X 2008 *Acta Phys. Sin.* **57** 1078 (in Chinese)
[22] Hou Q Y, Li J J, Ying Y C, Zhao C W, Zhao E J and Zhang Y 2013 *Chin. Phys. B* **22** 077103
[23] Lu J G, Fujita S and Ye Z Z 2007 *J. Appl. Phys.* **101** 083705
[24] Roth A P, Webb J B and Williams D F 1981 *Solid State Commun.* **39** 1269
[25] Sarkar A, Ghosh S, Chaudhuri S and Pal A K 1991 *Thin Solid Films* **204** 255
[26] Reynolds D C, Look D C and Jogai B 2000 *J. Appl. Phys.* **88** 5760
[27] Walsh A, Juarez L F, Silva S D and Wei S H 2008 *Phys. Rev. B* **78** 075211
[28] Lucarini V, Saarinen J J, Peiponen K E and Vartiainen E M 2005 *Kramers–Kronig Relations in Optical Materials Research*, Springer Series in Optical Sciences, Vol. 110 (Berline/Heidelberg: Springer Science + Business Media) pp. 27–35, ISBN: 978-3-540-23673-3 (print), 978-3-540-27316-5 (online)
[29] Tauc J, Grigorovici R and Vancu A 1966 *Phys. Status Solidi* **15** 627
[30] Sernelius B E, Berggren K F, Jin Z C, Hamberg I and Granqvist C G 1988 *Phys. Rev. B* **37** 10244
[31] Burstein E 1954 *Phys. Rev.* **93** 632
[32] Moss T S 1954 *Proc. Phys. Soc. London Sect. B* **67** 775
[33] Lu J G, Fujita S, Kawaharamura T, Nishinaka H, Kamada Y and Ohshima T 2006 *Appl. Phys. Lett.* **89** 262107